Tilted ab-axes MgB₂ films with high T_c and anomalous upper critical field anisotropy

Patrick A. Rondomanski, Autumn Heltman, Jack Glaser, Joan M. Redwing, and Qi Li

Abstract— MgB₂ is the highest transition temperature s-wave superconductor in ambient pressure with $T_c \sim 39$ K. It has a layered structure with two superconducting gaps, where the larger gap is confined in two-dimensional planes perpendicular to the c-axis [1], [2], [3], [4], [5]. Recently, it has been observed that MgB₂ displays Dirac nodal lines along the ab-axes, making it a potential topological superconductor [6], [7]. For probing many of these unique properties, MgB2 films with ab-axes exposed on the film surface are desirable. Recently, MgB2 [102] oriented films with bidirectional tilted c-axis have been fabricated on M-plane sapphire substrate using a HPCVD technique [8]. In this paper, we report the effect of the bidirectional grain structure in the [102] films on the anisotropy of H_{c2} with the current applied in two directions: parallel to the a-axis, $I_{\parallel a}$, and perpendicular to $I_{\parallel a}$ noted as $I_{\perp a}$, respectively. For $I_{\parallel a}$, two H_{c2} maxima were observed when the magnetic field is applied parallel to the ab-axes of either of the bidirectional grains, which is at the offset angles of $\pm 34^{\circ}$ from the field parallel to the surface direction. Only one H_{c2} maximum was observed at the applied field parallel to the film surface for $I_{\perp a}$. Notably, there is a local H_{c2} minimum at the field parallel to the surface for $I_{\parallel a}$. The observed phenomena can largely be explained by the bidirectional orientation of the tilted grains. These results demonstrate the importance of crystallographic orientation of thin films on the physical properties of MgB₂.

Index Terms—Anisotropic superconductivity, High transition temperature, High upper critical magnetic field, Hybrid physical-chemical vapor deposition, Magnesium diboride

I. INTRODUCTION

HE BCS superconductor magnesium diboride (MgB₂) is renowned for its high transition temperature (T_c ~39 K) in the bulk, with the greatest T_c of 41.8 K observed in HPCVD-grown epitaxial thin films on SiC [9]. Having sheets of graphitic-like boron sandwiched between closepacked Mg, MgB₂ retains a hexagonal crystal structure (P/6mmm, a= 3.06 Å, c= 3.52 Å). The layered structure results in well documented anisotropy of the physical properties [1], [10], [11], [12], [13], [14], [15], [16], [17]. Most notably, the upper critical field (H_{c2}) differs when the applied magnetic field is aligned to the ab-axes or to the c-axis, the latter being lower.

MgB₂ is a two-gap superconductor, with a larger energy gap of \sim 7.1 meV, due to the σ band contributions, and a smaller

energy gap of ~2.3 meV, due to the π band contributions [1], [2], [3], [4], [5]. The σ band carriers are largely confined to the C-plane (001) and the π band carriers dominate contributions along the c-axis direction. Additionally, along the a-axis {100} Dirac nodal lines, a topological band, have been observed in single crystals [6], [7]. Therefore, a MgB₂ film with the ab-axes normal to the substrate would allow access to the higher energy gap and the prospect of probing topological superconductivity. Toward this end, efforts have been made on the synthesis of tilted ab-axes films [4], [16], [18], [19].

1

There have been few studies toward synthesis of tilted *ab*-axes films and the tilt angles were relatively small, for example 19° on miscut MgO and 32° on YSZ substrates [4], [16], [18], [19]. The influence of the different grain orientations on H_{c2} in these films have not been studied in detail. Without yet achieving a {100} film, investigations of films with tilted *ab*-axes may offer some insight on the properties along those directions.

In this report, we explore the impact of MgB₂ [102] film orientation and bidirectional crystal grains on the H_{c2} anisotropy. We found that the anisotropy of H_{c2} in these films is strongly influenced by the tilted bidirectional grain orientations. All samples were patterned into two strips with perpendicular current directions, i.e. one along the a-axis and the other across the a-axis as well as the bidirectional grains. The maximum H_{c2} peak positions and the characteristic angular dependence were observed to differ significantly between the two strip directions. These results reflect the contributions to the H_{c2} anisotropy from the crystallographic orientation and bidirectional crystal grains in the films.

II. EXPERIMENTAL

The MgB₂ films in this study were synthesized by hybrid physical-chemical vapor deposition (HPCVD). The synthesis procedures have been described before [8], [9]. MgB₂ deposition on M-plane (100) Al₂O₃ produces films with a [102] axis normal to the substrate that tilts the c-axis by $\sim \pm 34^{\circ}$. The nominal film thickness is ~ 150 nm, measured at the valleys between grains from the cross-sectional TEM. For electrical measurements, two ~ 1 mm wide strips perpendicular to each

Manuscript receipt and acceptance dates will be inserted here. Magnetotransport measurements of this work are supported by the Department of Energy under Grant No. DE-FG02-08ER46531. The synthesis of the materials is supported in part by the National Science Foundation under the Graduate Research Fellowship Program (Grant No. DGE1255832) and DMR-1808900 and 1905833. Any opinions, findings, and conclusions or recommendations expressed in this material are those of the author(s) and do not necessarily reflect the views of the National Science Foundation. (Corresponding author: Qi Li.)

P.A. Rondomanski and J.M. Redwing are with the Department of Materials Science and Engineering, Pennsylvania State University, University Park, PA 16802, USA.

A. Heltman, J. Glaser, and Q. Li are with the Department of Physics, Pennsylvania State University, University Park, PA 16802, USA (qil1@psu.edu).

Color versions of one or more of the figures in this article are available online at http://ieeexplore.ieee.org

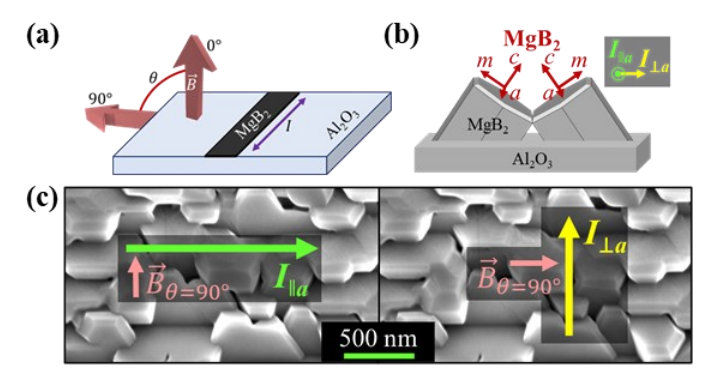


Fig. 1. (a) Experimental setup with current direction relative to magnetic field \vec{B} angle. (b) Schematic of the bidirectional crystal grains, the relative crystal axes and the two current directions. (c). Two strip patterning for the two current directions relative to the film morphology and the tilted grains.

other were patterned using a shadow mask and Ar ion milling on the same film cut into two halves. One strip was patterned parallel to the a-axis depicted in Fig. 1(b) (c, left). The other strip was patterned perpendicular to the a-axis and the bidirectional grains depicted in Fig. 1(b) (c, right). The tilted grain orientation was pre-determined before patterning using SEM images. During the measurement, the magnetic field (B)was always kept perpendicular to the current direction as shown in Fig. 1(a), while the magnetic field angle was varied. The two directions of the current relative to the tilted MgB2 grain are shown in Fig. 1(b)(c). The common ab-axes definition is relabeled as the m-axis (pointing at flats of the hexagon) or aaxis (pointing at corners of the hexagon) for the directions that correspond to the M-planes or A-planes, respectively. Depicted in Fig. 1(c), when the current follows along the a-axis of the MgB₂ grain, we refer to it as $I_{\parallel a}$. When the strip, thus the current, is perpendicular to $I_{\parallel a}$ direction across the bidirectional grains, we refer to it as $I_{\perp a}$.

The surface morphology of the films was assessed using a scanning electron microscopy (SEM). Electrical measurements were performed in a Quantum Design Dynacool or Evercool PPMS systems with the maximum field 14 T and 9 T, respectively, using a four-probe measurement. H_{c2} values were derived via measuring resistance as a function of applied field at fixed angles. H_{c2} was defined at 90% normal state resistance (R_n) as shown in Fig. 2 inset. From the resistance as a function of temperature curves, T_{c2} was defined at 90% R_n.

III. RESULTS AND DISCUSSION

Fig. 2 shows the dependence of H_{c2} on the magnetic field direction for the two current directions, $I_{\parallel a}$ and $I_{\perp a}$ at 12 K. For $I_{\parallel a}$, we see two H_{c2} maxima at the field angles of approximately $56^{\circ} \pm 3^{\circ}$ and $124^{\circ} \pm 3^{\circ}$, which correspond to the magnetic field direction parallel to the a-axes of the two orientations of the bidirectional tilted grains as shown in Fig. 1(b) and (c). This is consistent with the H_{c2} maximum in single crystals with the field parallel to the ab-axes, albeit it is now physically rotated 34° relative to the substrate surface. There is a H_{c2} minimum when the \vec{B} field is perpendicular to the substrate, at 0° and

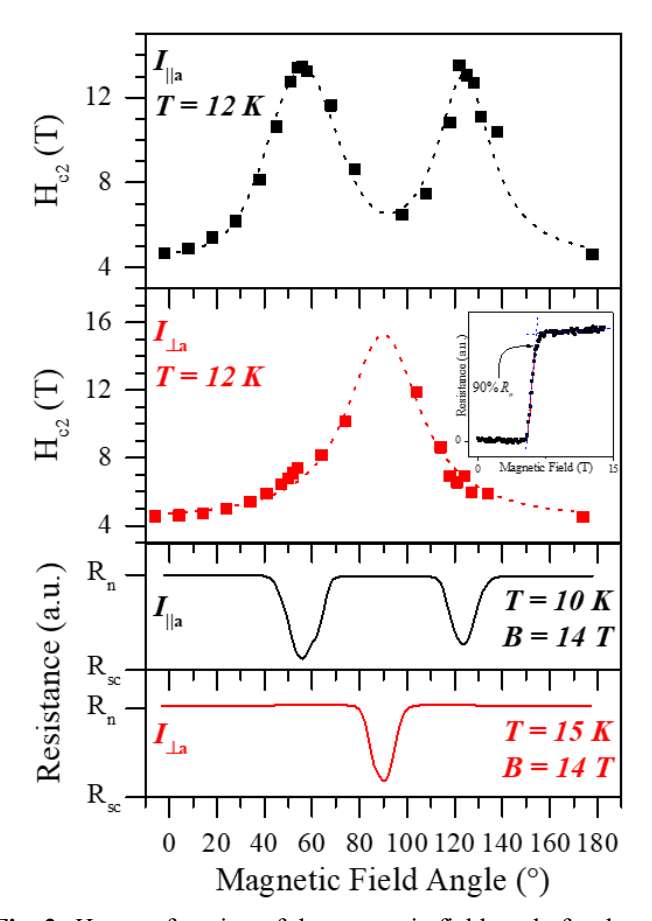


Fig. 2. H_{c2} as a function of the magnetic field angle for the two current directions. The opposing twinned grain orientation is evident by the two peaks for $I_{\parallel a}$. However, for $I_{\perp a}$, a single maximum at the field parallel to the surface is obtained. H_{c2} was determined as 90% normal resistance (R_n) as shown in the inset. Resistance as a function of angle for the two current directions are also shown in the two lower panels.

180°, and there is also a local minimum when \vec{B} is parallel to the substrate, at 90°. Normally, H_{c2} is maximum when \vec{B} is parallel to the film surface due to the thin film anisotropy or aligned with ab-axes in a single crystal due to crystal anisotropy, and there are minima when \vec{B} is perpendicular to the surface of a thin film or when \vec{B} is aligned with the c-axis of a crystal [15], [20], [21], [22]. For these [102] films, the \vec{B} field aligns with the c-axis at approximately 34° and 146° for the two orientations of the tilted grains. However, there are no H_{c2} minima at these angles. Where normally there should be a H_{c2} maximum at 90° for c-axis thin films, there is instead a local minimum, as seen in Fig. 2 $I_{\parallel a}$. Evidently, the orientation of the grains and the bidirectional grains within the film primarily contribute to the H_{c2} anisotropy. We have tried to use two anisotropic Ginzburg-Landau H_{c2} equations with an off-set angle to fit the curves in Fig. 2, but we find that the data does not fit well, suggesting that additional factors may also be influencing the anisotropy in a minor capacity.

To serve as a guide to the eye, a curve of best fit was drawn to show H_{c2} as a function of angle in Fig. 2. The anomalous H_{c2} anisotropy is further supported by the resistance as a function of angle results shown in Fig. 2, lower panel. Similar peak shape

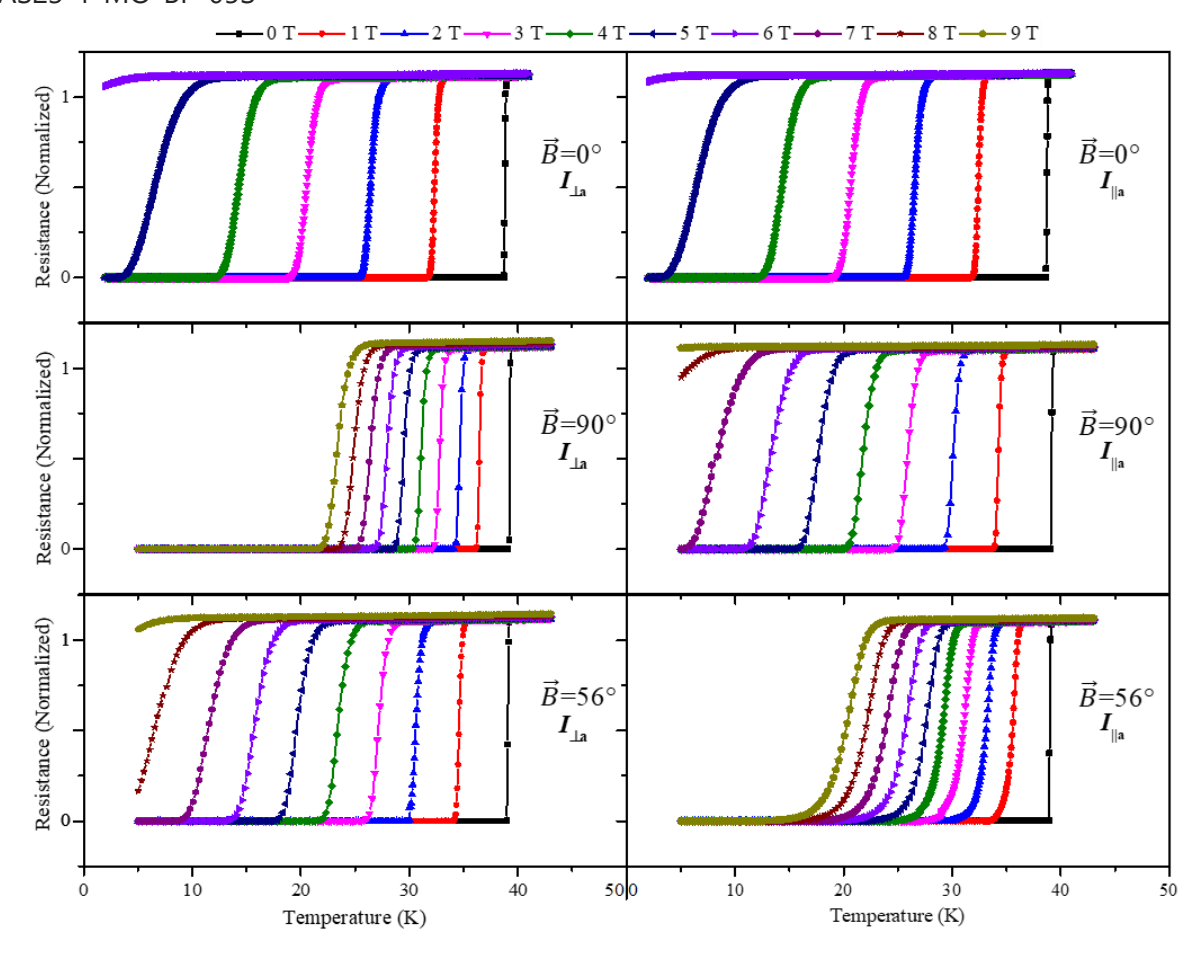


Fig. 3. Resistance superconducting transition curves for different magnetic fields at the min/max peak angles in Fig. 2. The left panel displays the results for $I_{\perp a}$ and the right panel displays the results for $I_{\parallel a}$. Note the similarities between the maximum H_{c2} peak positions for $90^{\circ}_{\perp a}$ (left) and $56^{\circ}_{\parallel a}$ (right). The y-axis is normalized for clarity.

and identical peak and valley positions between R and H_{c2} v.s angle plots are clearly seen.

Next, we examine the second plot in Fig. 2 for $I_{\perp a}$ where the sample patterning is turned 90° such that \vec{B} rotation does not align well with any of the major crystal planes for MgB₂ except in the parallel field direction where the field is parallel to the aaxis. Resembling results of a c-axis film, we observe a single maximum and minimum when the field is parallel or perpendicular to the surface, respectively. Again, a curve of best fit was drawn to serve as a guide to the eye. Here, the H_{c2} min and max are approximately 4.5 T and 14.4 T, respectively. The H_{c2} max value is lower than values obtained for pure c-axis films [19], [23], implying that even though the field is parallel to the ab-axes in this direction, other factors may also affect the H_{c2} value. The single maximum is also sensible considering that the magnetic field only aligns with the a-axis at this maximum peak angle and otherwise has no significant alignment with any MgB₂ crystal planes.

The resistance as a function temperature for different magnetic field values are shown in Fig. 3. The field angles of 0° (top), 90° (middle), and 56° (bottom) are measured for both strips with I_{La} (left) and $I_{\parallel a}$ (right). The angles are chosen based on the result of Fig.2. First the superconducting T_c is the same for both strips with the T_c about 39 K, indicating that the bidirectional grain boundaries and the film orientation did not

affect the T_c of the films. Unsurprisingly, at the perpendicular field direction (0°) the two datasets for the two current directions are nearly identical and the T_{c2} shows the largest drop with increasing field among the three angles measured. At 0°, the field direction for both current directions are identical and therefore the transition curves are identical, independent of the current direction. As expected from the H_{c2} peak angle seen in Fig. 2, for $I_{\perp a}$, T_{c2} displays the minimum drop with increasing field at $90^{\circ}_{\perp a}$, while for $I_{\parallel a}$, T_{c2} displays the minimum drop at $56^{\circ}_{\parallel a}$. For $I_{\parallel a}$, H_{c2} at $90^{\circ}_{\parallel a}$ is the local minima and is accurately reflected here with a T_{c2} decreases with the field less than that of the $0^{\circ}_{\parallel a}$ data but much greater than that of the $56^{\circ}_{\parallel a}$ data. For $I_{\perp a}$, on the other hand, $56^{\circ}_{\perp a}$ does not represent any crystal plane and hence does not show unusual behaviors. The significant difference of the two anisotropy curves for the two current strips reveals that multiple anisotropies, which are not aligned with each other, govern the final anisotropy curves.

From Fig. 2 and Fig. 3, we can see that the following anisotropy factors play roles in the results. For the $I_{\parallel a}$ strip, the layered crystal structure of MgB₂ results in a crystal anisotropy which would produce a H_{c2} maximum at 56° and minimum at 146°, corresponding to the field align with the a- or c-axes [11], for the [102] film. The bidirectional grains should also result in another H_{c2} maximum at 124° and minimum at 34°. This is the reason that we observed two maxima in Fig. 2. The crystal grain

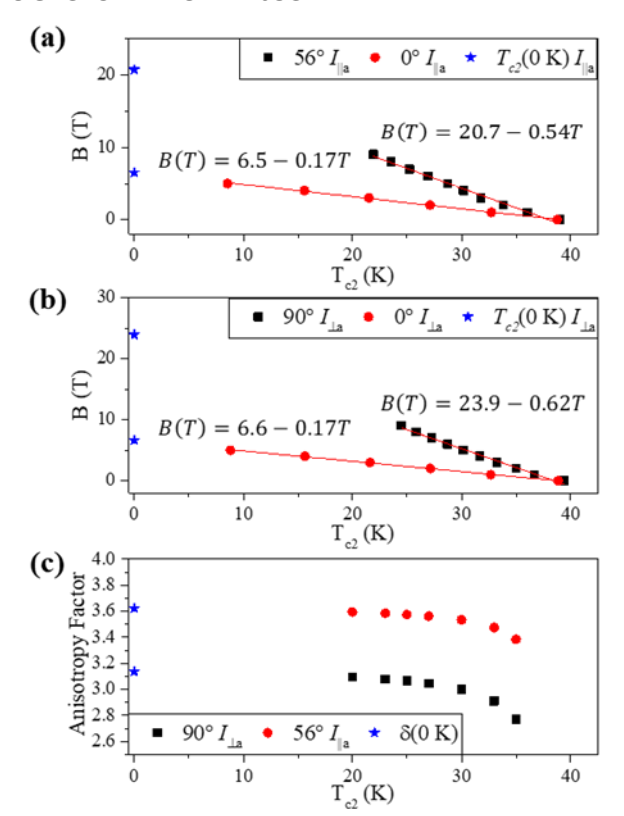


Fig. 4. Magnetic field as a function of T_{c2} for (a) $I_{\parallel a}$ and (b) $I_{\perp a}$. (c) Anisotropy as a function of T_{c2} . Extrapolations of the T_{c2} to T=0 K is marked.

orientation and the bidirectional grains are the major factors resulting in the final observed H_{c2} anisotropy. There are two maxima dominated by the crystal structure anisotropy for field parallel to the ab-axes. A local minimum at 90° is also dominated by combined crystal anisotropy of the bidirectional crystals. The minima at 0° and 180° are also dominated by the combined bi-crystals where our simulation using two crystal anisotropy with an off-set angle results in the same minimum. For the I_{La} direction, the sample rotation did not align with impactful crystal orientations to allow significant contributions from crystal anisotropy until it reaches 90° , so it displayed only one peak at the field parallel direction. Again, all these are evidence of the contributions from predominantly two anisotropic factors, influenced by the magnetic field angles relative to the grain orientations.

The next observation of Fig. 3 is that the T_c transitions in the $90^{\circ}_{\perp a}$ curve (Fig. 3 left) are sharper than those of the $56^{\circ}_{\parallel a}$ (Fig. 3 right) even though they both are at the H_{c2} maximum angle for the corresponding strip directions. There is a noticeable resistance broadening near zero resistance for the $56^{\circ}_{\parallel a}$ data (Fig. 3 right) which increases with increasing fields. Transition broadening may have many different origins [24], but in high magnetic fields at low resistance levels, it is normally governed by the vortex motions, especially thermally activated flux creep [20]. For thin film samples, the perpendicular component of the magnetic field roughly determines the vortex densities, and thus the corresponding resistance broadening due to the vortex motion. In a parallel field (90°), vortex formation parallel to the film surface is limited due to the thin thickness of the film and the surface and interface barrier limits the vortex motion in

that direction, while at $56^{\circ}_{\parallel a}$ even though it is the H_{c2} maximum, a substantial component of the perpendicular field generate vortices which can move within the film plane with the presence of a current. Thus, even though the H_{c2} maximum is observed at 56°_{\parallel} , the vortex motions still result in larger resistance broadening, especially near the tails of the transition, than that of the field parallel to the film surface for $I_{\perp a}$.

In Fig. 4(a-b), the applied magnetic field as a function of T_{c2} is plotted based on the data in Fig. 3. The H_{c2} is extrapolated using a first order polynomial fit of the data for both $I_{\parallel a}$ and $I_{\perp a}$, respectively. The projected $H_{c2}(0 \text{ K})$ for $I_{\parallel a}$ at 0° and 56° are 6.5 T and 20.7 T. The projected $H_{c2}(0 \text{ K})$ for $I_{\perp a}$ at 0° and $90^{\circ}_{\perp a}$ are 6.6 T and 23.9 T. These H_{c2} values are on par with that of typical MgB₂ crystal result [22] although the anisotropy here is the result of the bidirectional grains instead of a simple crystallographic anisotropy. It should be noted that for the parallel field, the H_{c2} is less than that of the c-axis film [19], [23]. This is probably due to the fact that the c-plane is tilted and there are also other factors which affect the H_{c2} and its anisotropy. However, from Fig. 2 and 3 we can also conclude that films with larger ab-axes tilt angle will improve the perpendicular H_{c2} , and doping of elements, like carbon, can also significantly increase H_{c2} if the material is intended for use in high field devices [25].

From the data in Fig. 4(a-b), anisotropy factors, $\delta = H_{c2}/H_{c2}^{0^{\circ}}$, are derived and displayed in Fig. 4(c). H_{c2} here is the peak value at the corresponding angle for both current directions. The $\delta(0 \text{ K})$ value of 3.1 and 3.6 are obtained for $\delta(0 \text{ K})$ for the I_{La} , and $I_{\parallel a}$ strips, respectively. It should be noted that the magnetic field rotates toward different crystal directions for the two different current strips which resulted in the difference of δ due to crystal orientations. The variation in δ with temperature has been observed which is attributed to the multiband nature of the material previously [15]. Overall, the reported H_{c2} anisotropy factors for MgB₂ in different films and single crystals have a rather large range from 1.1 to 8 [1], [10], [11], [19], and our measured anisotropy values for tilted films are within that range.

IV. CONCLUSION

We have fabricated MgB₂ [102] thin films with tilted ab-axes in a bidirectional grain structure on the M-plane sapphire substrates. The tilted axis and bi-directional grains did not affect the T_c which is about 39 K in the films. The upper critical field as a function of magnetic field angle, and the superconducting transition at different magnetic fields for two current directions perpendicular to each other have been measured. The samples have displayed a unique anisotropy of H_{c2} that is dominated by contributions of crystal anisotropy due to the film orientation and bidirectional grains. Additional anisotropy due to other factors may also be present. The two bidirectional anisotropy factors combined predominately yielded the observed anisotropy. Tilted thin films present a unique opportunity to recognize the importance of crystallographic influences on anisotropy that should be considered in the development of future superconducting thin film materials and devices.

EUCAS23-1-MO-BP-05S

REFERENCES

- [1] X. X. Xi, "Two-band superconductor magnesium diboride," Rep. Prog. Phys., vol. 71, no. 11, p. 116501, Nov. 2008, doi: 10.1088/0034-4885/71/11/116501
- [2] F. Giubileo et al., "Two-Gap State Density in MgB 2: A True Bulk Property Or A Proximity Effect?," Phys. Rev. Lett., vol. 87, no. 17, p. 177008, Oct. 2001, doi: 10.1103/PhysRevLett.87.177008.
- [3] F. Bouquet, R. A. Fisher, N. E. Phillips, D. G. Hinks, and J. D. Jorgensen, "Specific Heat of Mg 11 B 2: Evidence for a Second Energy Gap," *Phys. Rev. Lett.*, vol. 87, no. 4, p. 047001, Jul. 2001, doi: 10.1103/PhysRevLett.87.047001.
- [4] K. Chen *et al.*, "Momentum-dependent multiple gaps in magnesium diboride probed by electron tunnelling spectroscopy," *Nat Commun*, vol. 3, no. 1, p. 619, Jan. 2012, doi: 10.1038/ncomms1626.
- [5] M. Iavarone et al., "Two-Band Superconductivity in M g B 2," Phys. Rev. Lett., vol. 89, no. 18, p. 187002, Oct. 2002, doi: 10.1103/PhysRevLett.89.187002.
- [6] K.-H. Jin, H. Huang, J.-W. Mei, Z. Liu, L.-K. Lim, and F. Liu, "Topological superconducting phase in high-Tc superconductor MgB2 with Dirac–nodal-line fermions," npj Comput Mater, vol. 5, no. 1, p. 57, Dec. 2019, doi: 10.1038/s41524-019-0191-2.
- [7] X. Zhou et al., "Observation of topological surface states in the high-temperature superconductor MgB 2," Phys. Rev. B, vol. 100, no. 18, p. 184511, Nov. 2019, doi: 10.1103/PhysRevB.100.184511.
- [8] P. Rondomanski et al., "Hybrid Physical-Chemical Vapor Deposition of Epitaxial (10-12) MgB2 Films on M-Plane (10-10) Sapphire," unpublished, 2024.
- [9] A. V. Pogrebnyakov *et al.*, "Enhancement of the Superconducting Transition Temperature of M g B 2 by a Strain-Induced Bond-Stretching Mode Softening," *Phys. Rev. Lett.*, vol. 93, no. 14, p. 147006, Sep. 2004, doi: 10.1103/PhysRevLett.93.147006.
- [10] V. G. Kogan and S. L. Bud'ko, "Anisotropy parameters of superconducting MgB2," *Physica C: Superconductivity*, vol. 385, no. 1–2, pp. 131–142, Mar. 2003, doi: 10.1016/S0921-4534(02)02293-1.
- [11] M. Xu et al., "Anisotropy of superconductivity from MgB2 single crystals," Appl. Phys. Lett., vol. 79, no. 17, pp. 2779–2781, Oct. 2001, doi: 10.1063/1.1413729.
- [12] S. L. Bud'ko, V. G. Kogan, and P. C. Canfield, "Determination of superconducting anisotropy from magnetization data on random powders as applied to LuNi 2 B 2 C, YNi 2 B 2 C, and MgB 2," *Phys. Rev. B*, vol. 64, no. 18, p. 180506, Oct. 2001, doi: 10.1103/PhysRevB.64.180506.
- [13] J. D. Fletcher, A. Carrington, O. J. Taylor, S. M. Kazakov, and J. Karpinski, "Temperature-Dependent Anisotropy of the Penetration Depth and Coherence Length of MgB 2," *Phys. Rev. Lett.*, vol. 95, no. 9, p. 097005, Aug. 2005, doi: 10.1103/PhysRevLett.95.097005.
- [14] H.-J. Kim, B. Kang, H.-S. Lee, and S.-I. Lee, "Measurement of the anisotropy ratios in MgB2 single crystals," *Physica B: Condensed Matter*, vol. 378–380, pp. 890–891, May 2006, doi: 10.1016/j.physb.2006.01.328.
- [15] M. Angst et al., "Temperature and Field Dependence of the Anisotropy of \$\mathrm{MgB}}_{2}\$," Phys. Rev. Lett., vol. 88, no. 16, p. 167004, Apr. 2002, doi: 10.1103/PhysRevLett.88.167004.
- [16] P. Orgiani et al., "Anisotropic transport properties in tilted c -axis MgB 2 thin films," Supercond. Sci. Technol., vol. 23, no. 2, p. 025012, Feb. 2010, doi: 10.1088/0953-2048/23/2/025012.
- [17] Z. Wang, W. Yang, K. Chen, X. Xi, and Q. Li, "Anisotropic high upper critical field in ultrathin MgB2 films". *IEEE Transactions on Applied Superconductivity*, vol. 33, no. 5, pp. 1-5, Aug. 2023, Art no. 8600205, doi: 10.1109/TASC.2023.3264173.
- [18] M. Iavarone et al., "Characterization of off-axis MgB2 epitaxial thin films for planar junctions," Appl. Phys. Lett., vol. 87, no. 24, p. 242506, Dec. 2005, doi: 10.1063/1.2140473.
- [19] C. Zhuang et al., "Clean MgB 2 thin films on different types of single-crystal substrate fabricated by hybrid physical-chemical vapor deposition," Supercond. Sci. Technol., vol. 22, no. 2, p. 025002, Feb. 2009. doi: 10.1088/0953-2048/22/2/025002.
- [20] M. Tinkham, Introduction to Superconductivity, 2nd ed. New York: Dover Publications, 2004.
- [21] C. Ferdeghini et al., "Angular dependence of magnetoresistivity in coriented MgBthin film," Eur. Phys. J. B, vol. 30, no. 2, pp. 147–151, Nov. 2002, doi: 10.1140/epjb/e2002-00369-4.

- [22] A. Rydh et al., "Two-band effects in the angular dependence of H c 2 of MgB 2 single crystals," Phys. Rev. B, vol. 70, no. 13, p. 132503, Oct. 2004, doi: 10.1103/PhysRevB.70.132503.
- [23] X. Zeng et al., "In situ epitaxial MgB2 thin films for superconducting electronics," Nature Mater, vol. 1, no. 1, pp. 35–38, Sep. 2002, doi: 10.1038/nmat703.
- [24] T. Masui, S. Lee, and S. Tajima, "Origin of superconductivity transition broadening in MgB2," *Physica C: Superconductivity*, vol. 383, no. 4, pp. 299–305, Jan. 2003, doi: 10.1016/S0921-4534(02)02049-X.
- [25] V. Braccini et al., "High-field superconductivity in alloyed Mg B 2 thin films," Phys. Rev. B, vol. 71, no. 1, p. 012504, Jan. 2005, doi: 10.1103/PhysRevB.71.012504.